



---

## STRESS CORROSION CRACKING IN STEAM GENERATOR SG 1000 UNDER LOW-RATE STRAIN

Alexander Kazantsev<sup>1</sup>, Vladimir Lovchev<sup>2</sup>, Dmitriy Gutsev<sup>3</sup>,  
Alexander Zubchenko<sup>4</sup>, Sergey Kharchenko<sup>5</sup>

<sup>1</sup>Chief of Materials Strength Department, TSNIITMASH, Moscow (kazantsev\_a\_g@mail.ru)

<sup>2</sup>Chief of Materials Science Department, Rosenergoatom, Moscow

<sup>3</sup>Chief Technologist, Materials Science Department, Rosenergoatom, Moscow

<sup>4</sup>Deputy Director, GIDROPRESS (Experimental Design Bureau), Podolsk

<sup>5</sup>Chief of Department, GIDROPRESS (Experimental Design Bureau), Podolsk

### ABSTRACT

The paper deals with a study of retarded strain corrosion cracking in the steam generators for VVER-1000 reactor (10GN2MFA steel) in high-temperature water with copper and iron oxide deposits.

To model such fractures laboratory tests were performed to study corrosion cracking of steel 10GN2MFA at low rate loading on cylindrical and compact specimens with the working surfaces that had contacted the deposits of copper and iron.

According to the data on the static tensile tests of cylindrical specimens boundaries were defined for retarded strain corrosion cracking (RSCC) depending on the water conditions, the level of temperature, strain rate and composition of the deposits. The value of relative necking of a tensile specimen was used as a parameter that characterizes the development of corrosion damage.

It was shown that the removal of deposits and increasing water pH to 9.2 reduces the risk of corrosion damage.

The results of low-rate cyclic loading tests (1cycle/day) have shown a significant decrease in cyclic strength of steel 10GN2MFA in the presence of deposits of copper oxide. The data from these tests were used to determine the parameters of the cycle fatigue equation.

According to the tests of compact specimens under static and cyclic loading a significant effect of deposits of copper and iron oxide on the characteristics of the fracture toughness and crack growth rate was determined.

### INTRODUCTION

The operation of steam generators made of 10GN2MFA steel and installed in power units with VVER-1000 reactors demonstrates a possibility of cracks in separate joints of the equipment accompanied with corrosion wear of significant amount of metal.

The zone where cracks can appear in the welded joint of collector-to-PGV-1000 steam generator housing (fillet R20) is shown on the fig. 1. The specific features of the design of this assembly makes it possible for the copper and iron oxides to accumulate near this fillet as the steam generator is in operation. The FEM-analysis of the stressed-strained state of this joint has shown that in the zone of corrosion crack origination, the strain rate is equal to  $10^{-6}$  -  $10^{-7}$  1/sec for the majority of design conditions, except for emergency ones.

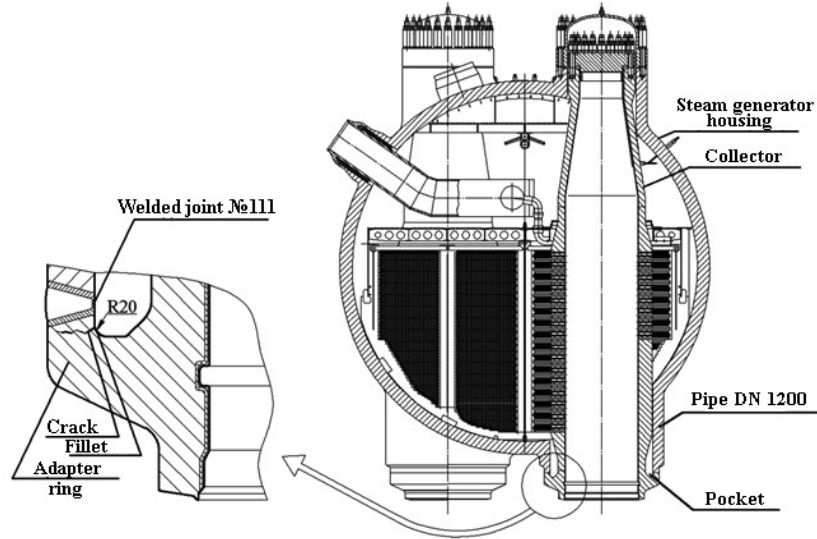


Figure 1. Collector-to-PGV-1000 steam generator housing welded joint

## TEST METHODS AND SPECIMENS

A program of laboratory tests was executed to study the conditions of appearance and development of cracks at slowly rate loading in more detail.

Tests were performed on smooth cylindrical specimens, 10 mm in diameter and compact specimens 20-25 mm thick with a fillet.

Cylindrical specimens were placed into a thin-walled sleeve of stainless steel, filled with deposits of specified content (Fig. 2). When testing the compact specimens with a fillet (Fig. 3) the fillet was filled up with deposits. The specimen with a fillet is more preferable to be tested as it is possible to trace both the moment the crack originates and the process of propagation in the same water chemistry (at least, at the initial stage). Thus, crack development begins with the corresponding initiating corrosion crack, not from an artificially created fatigue crack (induced by mechanical loading). Therefore, more adequate modeling of the conditions of real corrosion cracks development is thus provided.

Tests were performed in an autoclave, mounted on the test machine "Autograph" (Shimadzu).

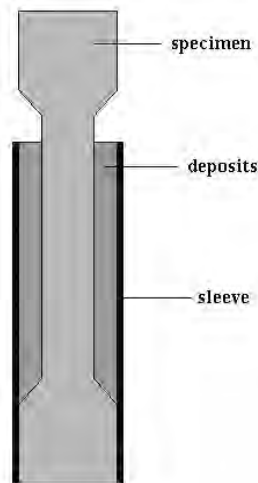


Figure 2. Tensile specimen with the working part contacting the deposits.

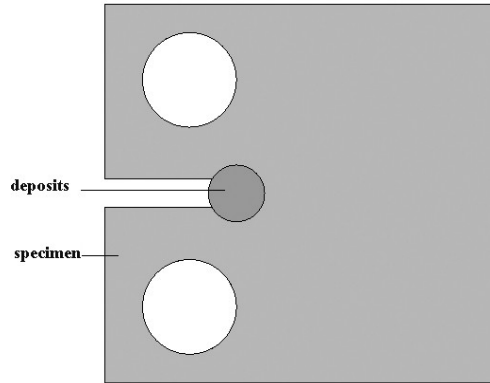


Figure 3. Compact specimen with a fillet filled up with deposits.

The water in the autoclave was preliminary bubbled with argon to remove the oxygen to the concentration  $[O_2] \leq 0.005$  mg/kg, to correspond to the primary coolant. Water temperature was equal to 100-300 °C, pH value at 25°C was in most cases assumed  $pH^{25} = 6$ .

The deposits were created by mixing  $Fe_2O_3$  and CuO powder. The main active component of the deposits, according to the tests, is CuO.

## RESULTS

The tests have shown that in a certain range of temperature and strain rates a drop of plastic properties takes place, and the specimen break with small deformations without plastic deformation necking. Corresponding dependences of the relative area reduction depending on the temperature and rate are presented in Fig. 4-5. At this, the deposits of content (75% of  $Fe_2O_3$  + 25% of CuO), typical of PGV-1000 collectors were used.

The minimum values of plasticity correspond to the temperature range of 180-290 °C and the strain rates of  $10^7$ - $10^6$  s<sup>-1</sup>. As soon as the strain rate increases to  $10^{-3}$  s<sup>-1</sup> the effect of corrosion cracking disappears. The behavior of the cracks that appear on the surface of the cylindrical specimen is displayed in Fig. 6.

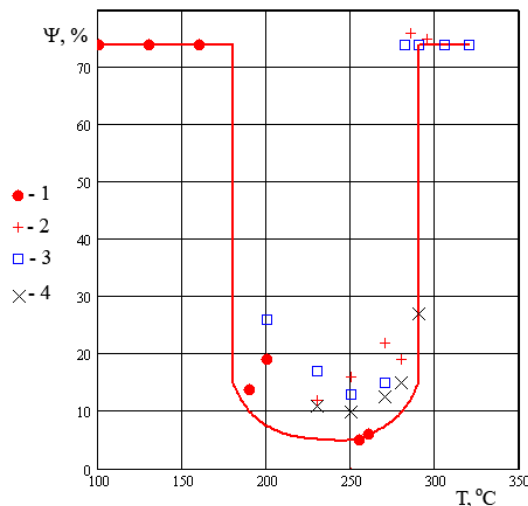


Figure 4. Effect of temperature on propensity of 10GN2MFA steel specimens to slow strain corrosion cracking in water at high parameters ( $\dot{\epsilon} = 1.4 \cdot 10^{-7} \div 3 \cdot 10^{-7}$  1/sec). 1 - bidistillate, deposits; 2 - bidistillate,  $[O_2] = 2$  mg/kg; 3 -  $[Na^+] = 0.5$  mg/kg;  $[Cl^-] = 0.5$  mg/kg;  $[O_2] = 4$  mg/kg; 4 - bidistillate,  $[O_2] = 4$  mg/kg.

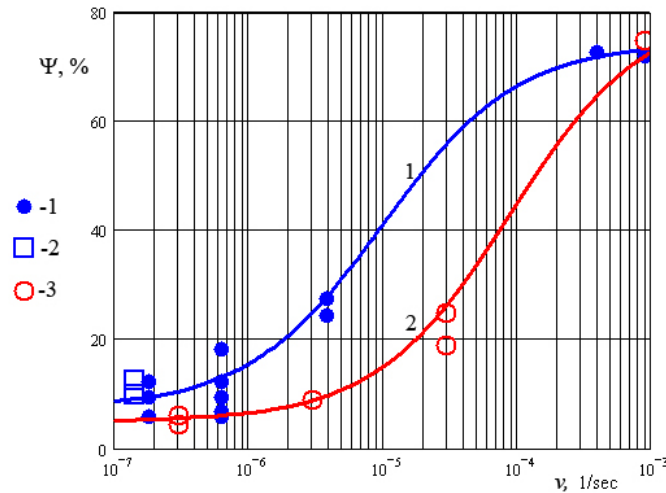


Figure 5. Dependence of necking on strain rate. 1, 2 - in water without deposits, pH = 4÷11, with oxygen up to 4 mg/kg, Fedorova V.A. et al. (2004); 3 - bidistillate, deposits.

The influence of the concentration of CuO and Fe<sub>2</sub>O<sub>3</sub> in the deposits on the value of necking of the specimen at fracture at strain rate  $\dot{\epsilon} = 3 \cdot 10^{-7}$  1/sec ( $T = 260$  °C) is given in Fig. 7. At least, until the value of CuO concentration reached 10% in oxygen-free water there was no RSCC observed, the specimens were broken with appearance of a “plastic neck” and the reduction of area reached  $\psi \approx 75\%$ . With CuO content from 25 % and above there is a drop of plasticity.

The research also covered a study of the effect of the thickness and length of deposit layer contacting with the specimen surface. When the thickness of deposit layer was reduced from 5 to 1 mm and the length of the zone of contact was reduced from 50 to 1 mm the effect of corrosion cracking remained.

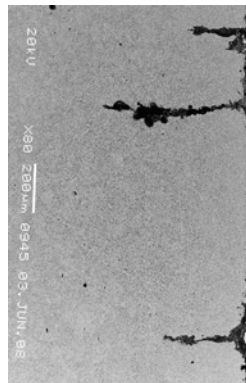


Figure 6. Corrosion cracks on the surface of a cylindrical specimen (increased 80-fold).

The presented results were obtained for  $\text{pH}^{25} = 6$ . Fig. 8 gives the influence of pH value on the curves of cylindrical specimen strain in water at  $T = 260$  °C in the presence of deposits of content (75% of Fe<sub>2</sub>O<sub>3</sub> + 25% of CuO). As  $\text{pH}^{25}$  increases from 6 to 8.5 the effect of corrosion cracking remained (curves 1-2), reduction of area  $\Psi = 12\%$ . At further increase of  $\text{pH}^{25}$  up to 9.2 the specimens got broken to viscous mechanism with the formation of the corresponding neck and without appearance of corrosion cracks, at the reduction of area of about 75% (curve 3). This data shows that due to growth of pH up to the required level, the effect of deposits, inducing corrosion cracking, can be neutralized. The content of water, used in tests, is presented in Tab.1.

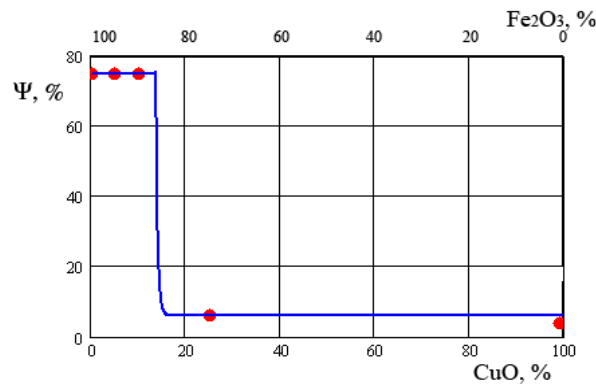


Figure 7. Influence of CuO concentration in deposits on the reduction of area of the specimen in tensile test (points - experimental data).

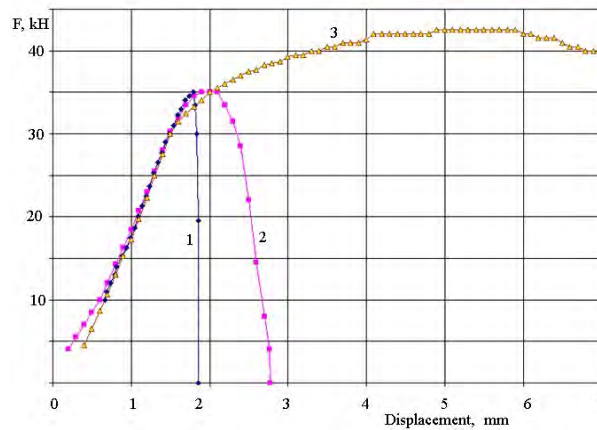


Figure 8. Diagrams of specimen tension in tests with variation of pH at  $T = 260\text{ }^{\circ}\text{C}$ .  
 1-  $\text{pH}^{25} = 6$ ; 2 -  $\text{pH}^{25} = 8.5$ ; 3 -  $\text{pH}^{25} = 9.2$ .

Table 1: Influence of water content on reduction of area of the specimens in tensile tests

Content and temperature of water	$\Psi$ , %
$T = 260\text{ }^{\circ}\text{C}$ . Bubbling, $\text{pH}^{25} = 6$ . Deposits 75% of $\text{Fe}_2\text{O}_3$ + 25% of $\text{CuO}$ ,	8
$T = 260\text{ }^{\circ}\text{C}$ . Bubbling + hydrazine 100 $\mu\text{g}/\text{kg}$ , deposits 75% of $\text{Fe}_2\text{O}_3$ + 25% of $\text{CuO}$ , $\text{pH}^{25} = 8.5$ .	12
$T = 260\text{ }^{\circ}\text{C}$ . Bubbling + ethanolamine 3.5 $\text{mg}/\text{kg}$ and hydrazine 20 $\mu\text{g}/\text{kg}$ , deposits 75% of $\text{Fe}_2\text{O}_3$ + 25% of $\text{CuO}$ , $\text{pH}^{25} = 9.2$ .	75

In the course of preventive maintenance of steam generators the specialists carry out chemical flushing to clean the internal surface of the collector in the zone of the mentioned fillet from deposits. To estimate its efficiency simulation tests were performed. Fig. 9 presents a diagram of specimen tensile test, recorded for the loading combined with flushing. At the first stage (the short interval of the strain diagram) the specimen with the deposits was tested until it reached the level of strain, not exceeding the ultimate strain (the moment the crack appears). Then the specimen was unloaded, cleaned and at the second stage it was tested until it was broken in bidistillate bubbled with argon without deposits (the long

interval of the strain diagram). There were no visible cracks on the surface of the specimen after the 1st loading. The diagrams of the 1st and 2nd stages in Fig. 9 were superposed in the origin of coordinates.

After flushing the viscous mechanism of fracture with neck formation was observed. The reduction of the area depended on the pre-strain level at the 1st stage and was equal to 20÷60%, Tab.2. The most important result is, that even when the 1st stage of loading took place only in the elastic area of the diagram, at subsequent post-flushing loading a decrease in plasticity was observed. It means that at low-rate strain the material is also damaged in the elastic strain areas.

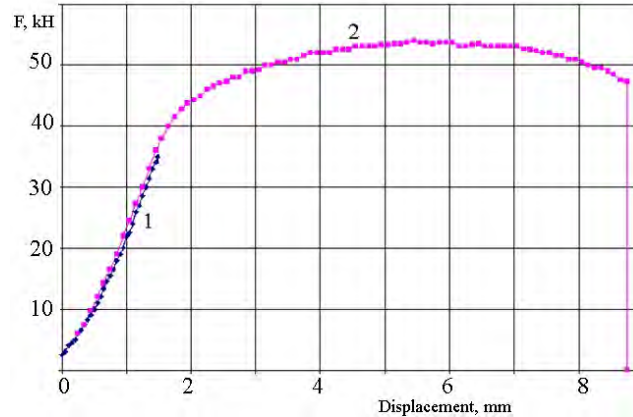


Figure 9. Diagrams of tension at combined loading with deposits (1) and after flushing (2).

Table 2: Results of combined tests with flushing.

Tests with flushing			
No	$\epsilon_{1p}, \%$	$\epsilon_{2p}, \%$	$\Psi, \%$
1	0.159	15	46.5
2	0.223	12	35
3	0.429	7.5	20
4	1.84	10	32
Test with flushing and finishing			
5	0.19	20	62

The positive effect is observed when the surface of the specimen is finished after flushing with removal of a layer of metal 3  $\mu\text{m}$  thick. In this case the plasticity of the specimen is close to the initial value. Tab.2  $\epsilon_{1p}$  and  $\epsilon_{2p}$  gives the plastic strains of the specimens at the 1st and 2nd stages of loading.

To create the conditions, inducing corrosion cracking in compact specimens with fillets, the tests were performed at the grip rate  $v = 1 \mu\text{m}/\text{min}$ . According to FEM-analysis in this case the rate of local strains in the apex of the mentioned fillet is equal to  $1.5 \cdot 10^{-6} \text{ 1/sec}$ . It follows from Fig.5 that the effect of a drop of plasticity at such strain rate is obvious.

In Fig.10 the curves of the strain of compact specimens with fillets are displayed at various conditions of loading (in terms “load - grip displacement”). At low-rate loading of  $1 \mu\text{m}/\text{min}$  in contact with the deposits in oxygen-free water the process is described by curve 1; without deposits in water with oxygen content of 4.5 mg/kg – by curve 2; at higher rate of strain (1 mm/min) with deposits – by curve 3.

At low-rate loading in the top of the fillet corrosion cracks without significant plastic deformations of the specimen was observed. Significant plastic deformations of the specimens and their necking were detected in the tests with loading rate of 1 mm/min though there were no cracks.

According to these tests JR curves (Fig. 11) were plotted with the use of the method of compliance (under conventional conditions of loading) - curve 1, and a multi-specimens method (at low-rate loading with deposits) - curve 2.

In Fig. 11 the significant drop of fracture toughness in the conditions of low-rate loading with deposits is obvious.

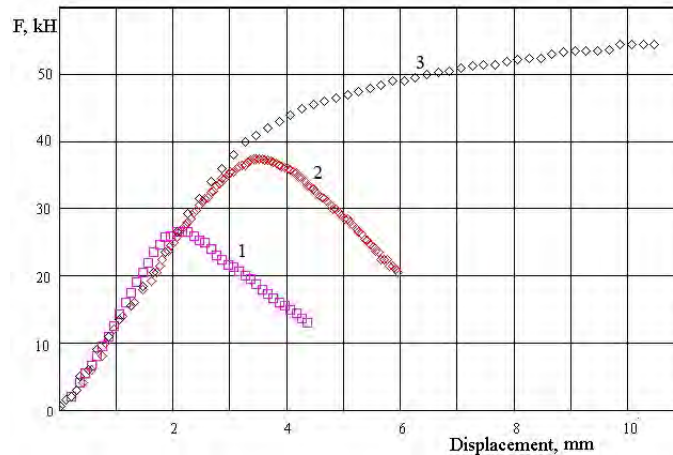


Figure 10. Strain diagrams of compact specimens with a fillet at  $T = 260\text{ }^{\circ}\text{C}$ ,  $\text{pH} = 6$ .  
 1 -  $\nu = 1\text{ }\mu\text{m}/\text{min}$ , with deposits; 2 -  $\nu = 1\text{ }\mu\text{m}/\text{min}$ ,  $[\text{O}_2] = 4.5\text{ mg}/\text{kg}$ , without deposits;  
 3 -  $\nu = 10^3\text{ }\mu\text{m}/\text{min}$ , with deposits.

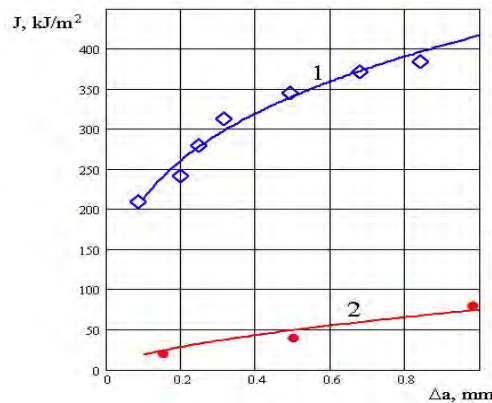


Figure 11. J-R curves for steel 10GN2MFA loaded at the rate of 1mm/min (1) without deposits and at low rate of 1  $\mu\text{m}/\text{min}$  with deposits (2).

A possibility of corrosion cracking of steel 10GN2MFA at low-rate cyclic loading at contact of specimens with deposits of content (25% of  $\text{CuO} + 75\%$  of  $\text{Fe}_2\text{O}_3$ ) was also studied in the work.

The loading was carried out with the stress ratio  $r = 0$ . The rate of loading in the tension semi-cycle was assumed to be similar to that in case of the static stress at RSCC, i.e. about  $3 \cdot 10^{-7}$  1/sec. The unloading was carried out at higher rate to decrease the labor content of tests. The duration of the cycle was approximately equal to one day.

The value of maximum stress was set in the range of 0.8-1.0 of the yield strength. The corresponding results of the tests (in amplitudes of stress) are represented in the Fig. 12 (points 3).

The same figure shows (in amplitudes of conditional stresses) experimental data for steel 10GN2MFA (hard loading) in the absence of corrosion environment (points 1 and 2).

From the Fig. 12 it is obvious that the reduction of the amplitude of cyclic stress at low-rate loading for the given life depends on the level of stress, and can take place with a coefficient of up to 20. The obtained results can be presented by the Langer equation in the amplitudes of conditional stresses the way it is given in PNAE G-7-002-86 (1989):

$$\sigma_a^* = \frac{E \cdot e_c}{(4N_0)^{m_p}} + \frac{R_{-1}}{1 + \frac{R_{-1}}{R_m} \frac{1+r}{1-r}} \quad (1)$$

here  $E = 2 \cdot 10^5$  MPa - modulus of elasticity;  $e_c$  - parameter of plasticity, defined according to PNAE G-7-002-86 (1989);  $R_{-1} = 0.4 \cdot R_m$  - fatigue strength at a symmetric cycle of loading;  $R_m$  - ultimate strength;  $r$  - stress ratio;  $m_p = 0.5$ . The amplitude of conditional stresses is calculated from the equation  $\sigma_a^* = E \cdot \varepsilon_a$ , where  $\varepsilon_a$  - amplitude of elastic-plastic strains.

The effect of drop of plasticity in conditions of RSCC was taken into account by the equation

$$e_{c \text{ RSCC}} = e_{c \text{ air}} \frac{\varepsilon_{f \text{ RSCC}}}{\varepsilon_{f \text{ air}}},$$

here  $\varepsilon_{f \text{ air}}$  and  $\varepsilon_{f \text{ RSCC}}$  - limiting strains at tension in the air and at RSCC conditions.

In the Tab.3 values of parameters of the equation (1) are presented for the case of low-rate loading with deposits and also for loading in ambient conditions in the air. The calculated fatigue curves for tests in the air and in corrosion environment with deposits ( $r = 0$ ) are presented in the Fig. 12.

Table 3: Parameters of the fatigue curve equation

Loading conditions	$\varepsilon_f, \%$	$e_c, \%$	$R_{-1}, \text{MPa}$	$R_m, \text{MPa}$	$m_p$
in air	140	34.6	208	520	0.5
in water with deposits	0.68	0.168	178	450	0.5

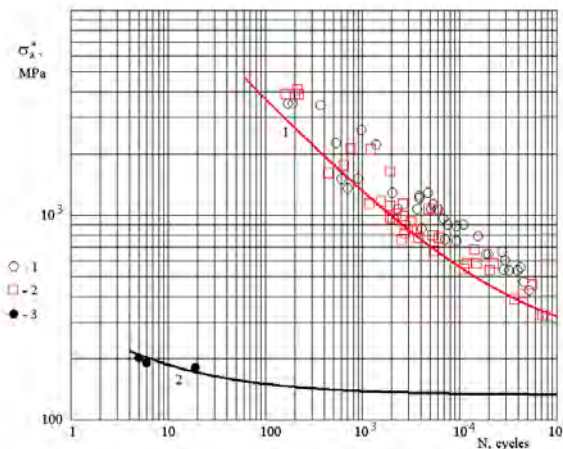


Figure 12. Fatigue curves for steel 10GN2MFA in the air (1) and at low-rate loading in water with deposits (2). Points - experimental data: 1 -  $T = 20$  °C, 2 -  $T = 350$  °C - in the air; 3 -  $T = 260$  °C at low-rate loading (1cycle/day) in water with deposits.

As follows from the Fig. 12, the results of calculations correspond to experimental data. The obtained results prove the possibility of plotting the fatigue curves at low-rate loading on the basis of static tests in corresponding conditions.

On the basis of testing the specimens with a fillet the estimation of the rate of crack growth was also obtained at low-rate cyclic loading at contact of working surface of the sample with deposits. Frequency of loading was equal to 1 cycles/day, the stress ratio  $r = 0$ . The compliance method was used to measure the length of cracks in an autoclave. Also the length of the cracks was measured using an optical microscope after cutting the tested specimens.

The results of the tests are presented in Fig. 13 in coordinates: fatigue crack growth rate – stress intensity factor range. The same figure shows results of tests in the air, in water with increased content of oxygen at various frequencies of loading according Matocha K. and Cicryt F. (2006), and also a curve according to the ASME Code.

It is obvious in Fig.13 that the presence of deposits leads to significant growth of crack rate in comparison with the tests in the air and in water without deposits.

For steel 10ГН2МΦА crack growth rate in the air is described by the Paris equation in the form  $da/dN = C \cdot (\Delta K)^m$ , where  $m = 2.7$ ;  $C = 2.8 \cdot 10^{-8}$ , RD EO 0330-01 (2004). Using the results of the tests the Paris equation parameters were defined for low-rate loading with deposits:  $m = 2.7$ ;  $C = 1.33 \cdot 10^{-4}$ , Tab.4. Here  $da/dN$  is in mm/cycle, and  $\Delta K$  is in  $\text{MPa} \cdot \text{m}^{0.5}$  units.

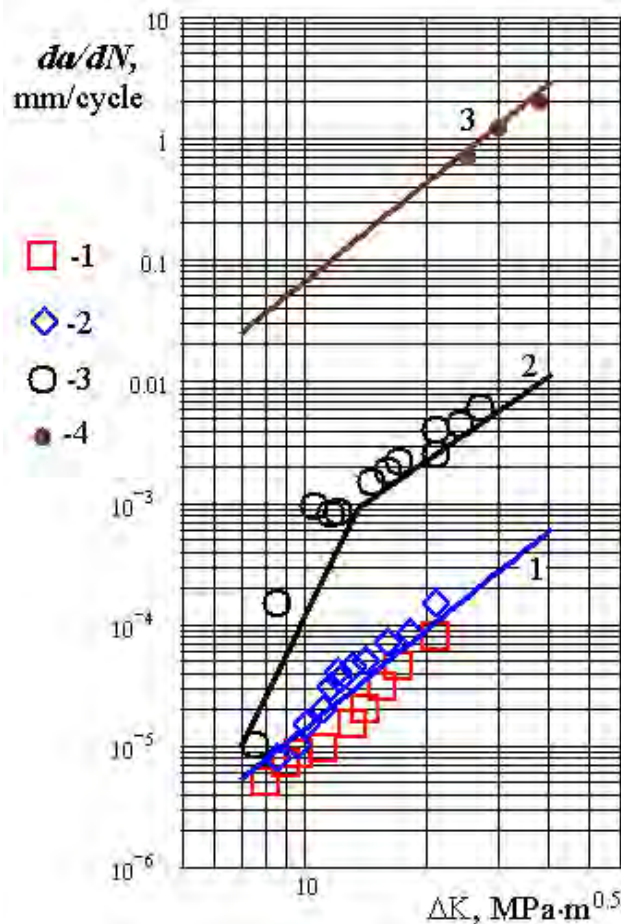


Figure 13. Fatigue crack growth behavior in 10GN2MFA steel in different environments.  
 Points: 1 - air, 20 °C,  $f = 1$  Hz,  $r = 0.5$ ; 2 - air, 290 °C,  $f = 0.1$  Hz,  $r = 0.7$ ; 3- water, 290 °C,  $f = 0.017$  Hz,  $r = 0.7$ , Matocha K. and Cicryt F. (2006); 4 - water with deposits, 260 °C,  $f = 1$  day/cycle,  $R = 0$ .  
 Curves: 1 - air,  $r = 0$ ; 2 - water, ASME CODE (2001); 3 - water with deposits, 260°C,  $f = 1$  day/cycle,  $r = 0$ .

Table 4: Parameters of the Paris equation

Test conditions	m	C
In air, $r = 0$	2.7	$2.8 \cdot 10^{-8}$
In water with deposits, $r = 0$	2.7	$1.33 \cdot 10^{-4}$

## CONCLUSION

On the basis of revealed laws of corrosion cracking of steel 10GN2MFA a series of measures to improve the working characteristics of the area of collector-to- PGV-1000 steam generator housing welded joint was offered, including a decrease of the level of stresses and elimination of the corresponding corrosion constituent.

Positive results can be achieved due to reducing the concentration of stresses in the area of the fillet and general loading of the zone, and also at improvement of the efficiency of flushing (removal of deposits from the area). The most cardinal solution of corrosion cracking problem is the elimination of the application of copper elements from the secondary side of nuclear power plants with VVER-type power reactors.

## REFERENCES

- Fedorova V.A., Margolin B.Z., Kostylev V.I. (2004). "Analysis of the possible causes of damage to the collector joint welding nozzle steam generator PGV-1000M". Abstracts of the 8-th Int. Conf. St. Petersburg - Sosnovy Bor, Russia, 60-61.
- Matocha K., Cicryt F.(2006). "The Simultaneous Effect of Ageing and Water Environment on Subcritical Crack Growth and Fracture Behaviour Of 10GN2NFA Low Alloy Steel". *Metallurgical Transactions A*, 11A, 21-30.
- Standards of strength analysis of equipment and pipelines of nuclear power plants. PNAE G-7-002-86.* (1989). Energoatomizdat, Moscow, Russia, 525 p.
- Tool to calculate the strength of equipment and piping reactors of RBMK reactors and EGP during the operational phase.RD EO 0330-01.* (2004). Federal Agency for Atomic Energy, Moscow, Russia.
- ASME Standards Boiler and Pressure Vessel Code.* (2001). New York, USA.